Available online at www.sciencedirect.com
ScienceDirect
Trans. Nonferrous Met. Soc. China 33(2023) 383−395
Transactions of Nonferrous Metals Society of China
www.tnmsc.cn

Preparation of high performance 5083 aluminum alloy by alternate ring-groove pressing and torsion

Yong-fei GU[1], Wei-peng LIU[1], Hao-shan GUO[1], Chun-xiang ZHANG[2], Jun-ting LUO[1,2]

1. Key Laboratory of Advanced Forging and Stamping Technology and Science, Ministry of Education, Yanshan University, Qinhuangdao 066004, China;
2. State Key Laboratory of Metastable Materials Science and Technology, Yanshan University, Qinhuangdao 066004, China

Received 19 October 2021; accepted 30 March 2022

Abstract: A preparation process of high performance 5083 aluminum alloy sheet was proposed. The process is severe plastic deformation process of alternate ring-groove pressing and torsion based on cyclic stress state under warm conditions. The results show that when the temperature is 200 °C, the grain refinement effect after secondary deformation is the best, and the average grain size is refined from 24 to 12.5 μm. When the temperature is 300 °C, the mechanical properties of the sheet after one deformation are the best. Compared with those of the original sheet, the tensile strength (397 MPa) and breaking elongation (28.3%) are increased by 30% and 60%, respectively. The second phase particles and recrystallized grains improve the strength of the material by second phase strengthening and fine grain strengthening. The equiaxed recrystallized grains improve the plasticity and toughness of the material.

Key words: 5083 aluminum alloy; alternate ring-groove pressing and torsion; cyclic stress state; mechanical properties

1 Introduction

One of the methods to improve the mechanical properties of materials is to refine the grains (nanometer or submicron level). The decrease in grain size will improve the strength and toughness of the material at room temperature. Moreover, good formability and superplasticity may be obtained [1,2]. Severe plastic deformation is a better grain refinement process. Many severe plastic deformation methods, such as equal channel angular pressing [3], high-pressure torsion [4,5], accumulative roll-bonding (ARB) [6], and constrained groove pressing (CGP) [7], have been proposed. Among them, ARB [8] and CGP [9] are the maturer sheet grain refinement processes. The characteristic of ARB and CGP is that although the grains and lattice of material will be strongly fragmented and distorted after severe plastic deformation, the macroscopic size of the material even will keep unchanged state. The formation of a sub-crystalline structure with high dislocation density and defect density effectively refines the grains.

POURALIAKBAR et al [10−13] carried out restricted compression molding on stress-relieved Al−Mn−Si samples at the strains of 0.47, 0.80, and 1.27, respectively. The deformed sheets were subjected to isothermal heat treatment at 150, 250, and 350 °C, respectively. The cold rolled samples with a strain of 0.80 after two-pass die pressing and flattening had better performance, and the maximum uniform elongation was 22.96% after annealing at 350 °C. However, the strength decreased greatly because of subsequent annealing.

Corresponding author: Jun-ting LUO, E-mail: luojunting@ysu.edu.cn
DOI: 10.1016/S1003-6326(22)66114-4

KOTOBI et al [14,15] used the elastic-plastic relationship to estimate the deformation force in the restrictive molding process. The estimation results were compared with the experimental data and finite element simulation results. According to the results, the relationship can be used to predict the deformation force in the process of restrictive die pressing with different materials and different geometries. They compared von Mises yield criterion with that of Teresca and found that von Mises yield criterion can better estimate the deformation force in the restrictive molding process. WANG et al [9] studied the effects of groove width and angle on the properties of commercial pure nickel sheet in the CGP process through experiments and numerical simulation. They showed that the mechanical properties of a sheet sample with a thickness of 2 mm can be optimized through two-pass CGP with a groove width of 2 mm and a groove angle of 45°. The yield strength and tensile strength were 476.3 and 532.3 MPa, respectively; the elongation at break was 10.6%; the average hardness was HV 218.9. They found that the forming load of the CGP mold decreased exponentially with the groove width but was not affected by the groove angle.

5083 aluminum alloy has good plasticity, processability, moderate strength, excellent weld-ability and good corrosion resistance [16−18]. In this work, we proposed a new preparation process for high-performance 5083 aluminum alloy: alternate ring-groove pressing and torsion based on cyclic stress state at cold and warm temperatures. The process uses two sets of ring-groove mold and a set of flattening mold. Cold processing at room temperature can improve the strength of the sheet [19−21], and warm processing can keep the plasticity of the sheet [22]. In this process, the grain size of the sheet is refined by applying repeated tension–compression–torsion cyclic stress. The aluminum alloy sheet with fine-grained structure prepared by the process realizes the dual increase in strength and elongation.

2 Experimental

The experimental material was a 5083 aluminum alloy sheet with a thickness of 1.2 mm. Element compositions of 5083 aluminum alloy are shown in Table 1. In this experiment, a circular sheet with a diameter of 74 mm was cut by wire cutting. Cyclic compression–torsion test was carried out on a 500T hydraulic press with self-designed and manufactured torsion frock. The designed ring-groove molds are shown in Fig. 1. The center waves of ring-groove molds I and II have the same phase, whereas the rest of the ring-grooves have a certain phase difference. The trough and peak of ring-groove mold I correspond to the joint of the trough and peak of ring-groove mold II, respectively.

The proposed warm ring-groove with repeated molding–torsion process is shown in Fig. 2. The one-pass deformation process is as follows: molding with ring-groove mold I, torsion, torsion and flattening at room temperature; molding with ring-groove mold II, torsion, torsion and flattening at room temperature. Three temperature conditions (200, 250, and 300 °C) were used in the warm flattening process. Three test processes were set according to these temperatures (Process 1: flattening at 200 °C, 1–2 passes; Process 2: flattening

Table 1 Element compositions of 5083 aluminum alloy (wt.%)

Al	Mg	Mn	Si	Fe	Zn	Cr	Ti	Cu
Bal.	4.0−4.9	0.4−1.0	0.40	0.4	0.25	0.05−0.25	0.15	0.1

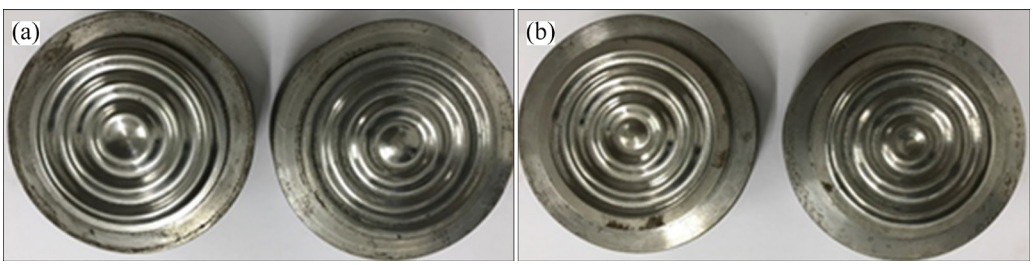

Fig. 1 Two sets of ring-groove mold: (a) Ring-groove mold I; (b) Ring-groove mold II

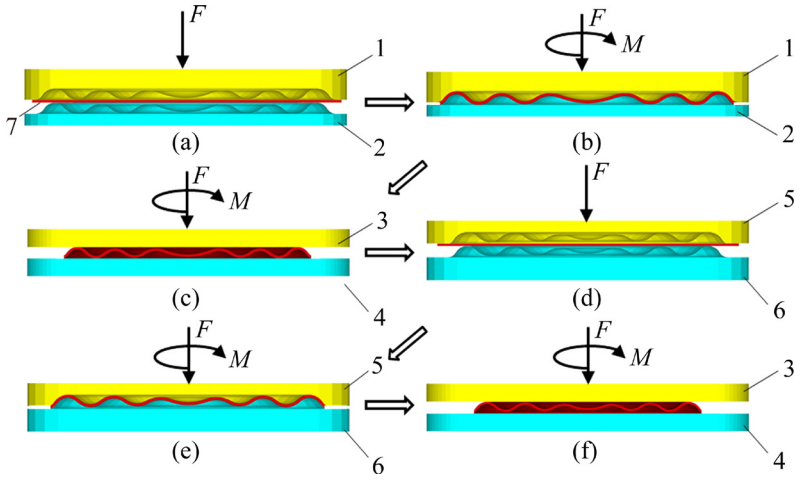

Fig. 2 Experimental procedure of annular-corrugation repetitive molding process: 1—Upper ring-groove mold I; 2—Lower ring-groove mold I; 3—Upper flattening mold; 4—Lower flattening mold; 5—Upper ring-groove mold II; 6—Lower ring-groove mold II; 7—Sheet

at 250 °C, 1–2 passes; Process 3: flattening at 300 °C, 1–2 passes). The symbolic representation of various processes is shown in Table 2.

Wire cutting was performed to cut the 5083 aluminum alloy sheets after different processes. Six 5 mm × 5 mm samples were obtained from the center to the outside of the circular sheet. The sampling positions are shown in Fig. 3. The samples were ground, polished, corroded, and then analyzed with a Zeiss Axio Scope A1 metallographic microscope. An MVS−1000D1 microhardness tester was used for hardness analysis. A wire cutting machine was used to cut tensile specimens in the tangential direction on the sheets processed by different processes, and the location is shown in Fig. 3. The electronic universal tensile testing machine was used to test the mechanical properties, and the tensile rate was $\dot{\varepsilon}=3.64\times10^{-4}$ s^{-1}. The tensile fracture morphology of the 5083 aluminum alloy sheets treated by different processes was analyzed by a Hitachi TM3030 scanning electron microscope.

Table 2 Symbolic representation of various processes

Process No.	Pass	
	1	2
1 (200 °C)	1-1	1-2
2 (250 °C)	2-1	2-2
3 (300 °C)	3-1	3-2

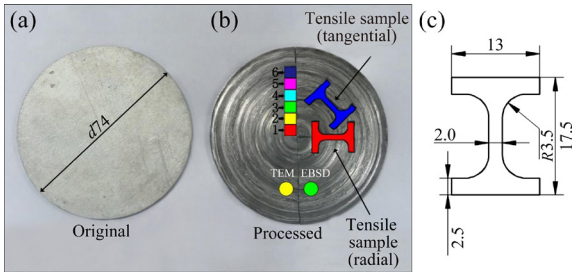

Fig. 3 Deformation zone and sampling position of sheet: (a) Original plate; (b) Sampling position; (c) Size diagram of tensile specimen (unit: mm)

3 Results and discussion

3.1 Microstructure

Commercial 5083 aluminum alloy sheet was adopted as the original sheet and then rolled and annealed in multiple passes during the production process. The microstructure of the original sheet is shown in Fig. 4. The average grain size of the

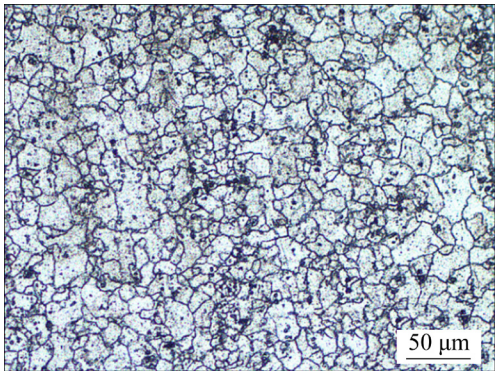

Fig. 4 Microstructure of original 5083 aluminum alloy sheet

original sheet is about 24 μm, but the grain size is not uniform with remarkable differences.

Six metallographic samples, numbered 1−6, were obtained from the center outward of the sheet. The metallographic structures under different molding torsion process conditions are shown as follows.

The metallographic structure of the sheet treated by Process 1-1 is shown in Fig. 5. Compared with the flattened tissue at room temperature, the vacancy diffusion, dislocation sliding, and dislocation rearrangement are obvious. Cross slip occurs under the interaction of thermal activation and stress. Thus, a cellular structure is formed with a grain size of 0.5−1 μm. Based on the metallographic situation reflected in each figure, the main softening mechanism is dynamic recovery because of insufficient thermal activation. The grain size of the dynamic recovery structure is between 10 and 20 μm, and the grains are equiaxed.

The dynamic recrystallization and dynamic recovery of the materials are thermal activation processes. However, the activation energy required for the directional migration of atoms for dynamic recrystallization is much higher than that required for dynamic recovery, which is caused by vacancy diffusion, edge dislocation climbing, and screw dislocation slippage [23−25].

The metallographic structure of the sheet processed by Process 2-1 is shown in Fig. 6. When

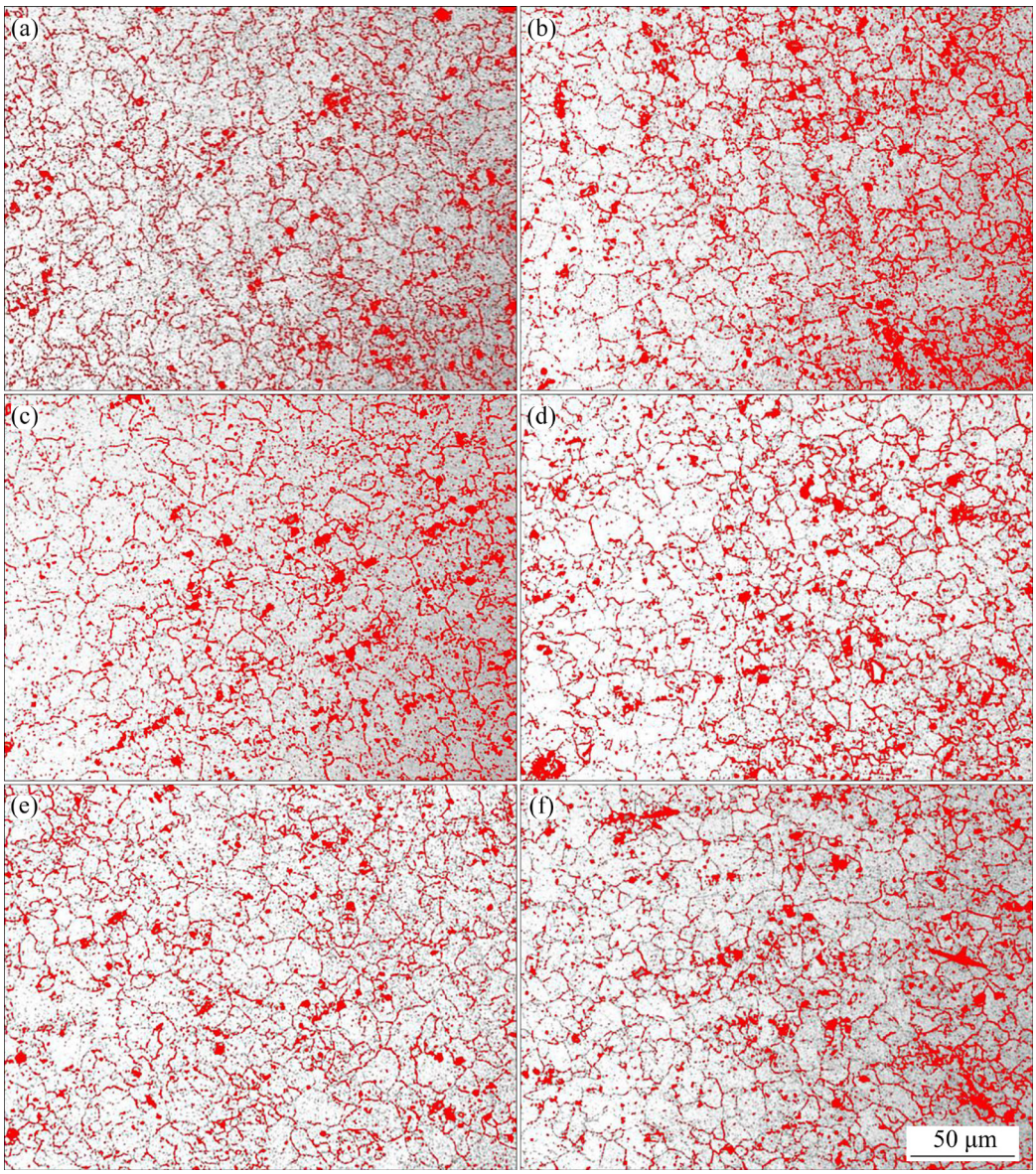

Fig. 5 Metallographic structure of sheet processed by Process 1-1: (a) Position 1; (b) Position 2; (c) Position 3; (d) Position 4; (e) Position 5; (f) Position 6

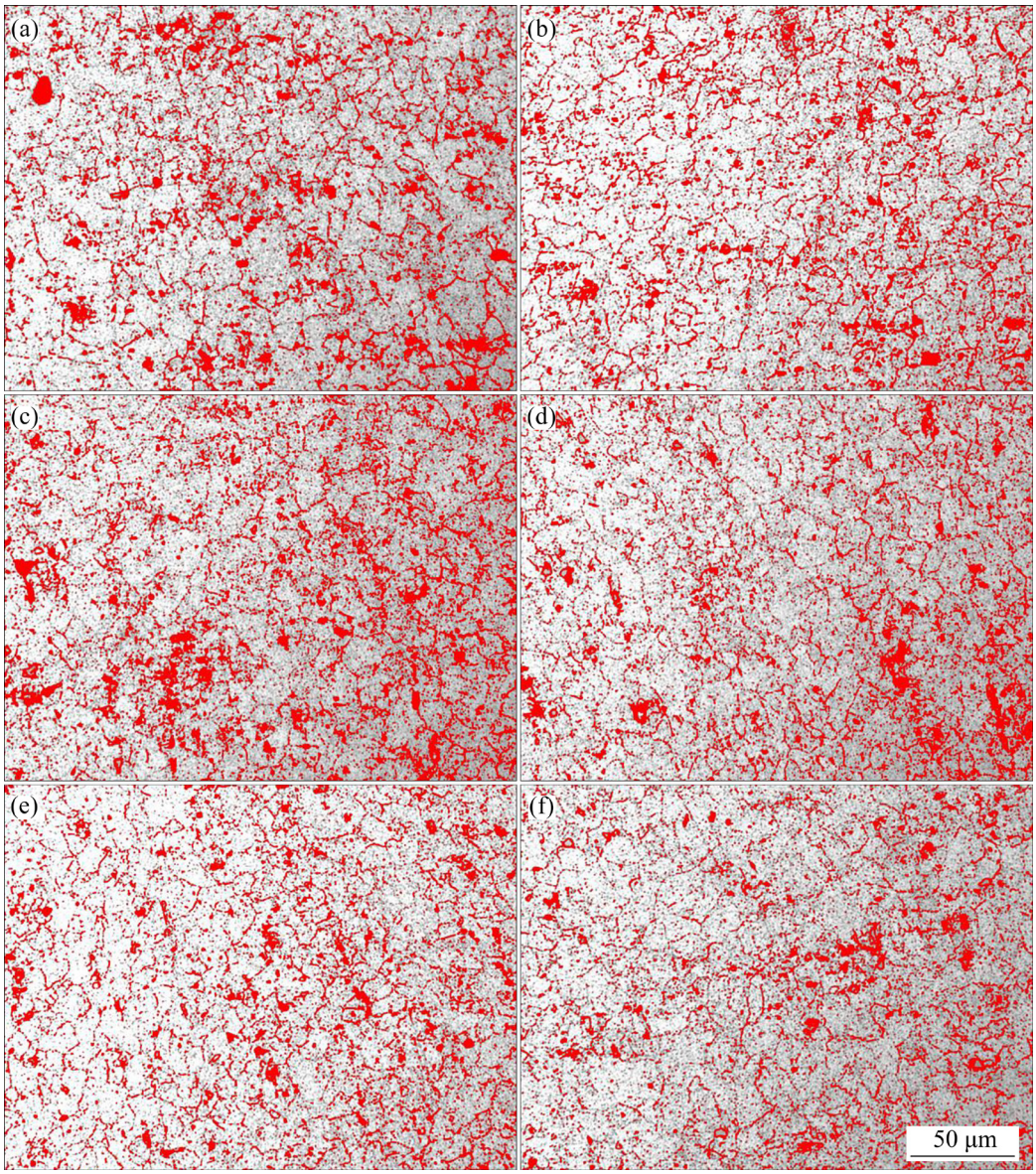

Fig. 6 Metallographic structure of sheet processed by Process 2-1: (a) Position 1; (b) Position 2; (c) Position 3; (d) Position 4; (e) Position 5; (f) Position 6

the final flattening temperature reaches 250 °C, about 20% of the dynamically recrystallized grains can be obtained. At this time, partial dynamic recrystallization is still in the initial stage of growth, and the grain size is small and belongs to the state of sub-dynamic recrystallization. The activation energy at 250 °C is enough to make the dislocation move to the sub-grain boundary in a short time. The β phase is preferentially precipitated at the intersection point between the sub-grain boundary and grain boundary. The β phase has a relatively uniform point-like distribution in the figure. At this time, the material softens under the coordinated action of dynamic recovery, recrystallization, and other processes. As a result, the average grain size reaches 15.5 μm.

The metallographic structure of the sheet processed by Process 3-1 is shown in Fig. 7. The average size of sheet grains reaches 18 μm. This occurrence is due to the moderate deformation of the material and the high temperature environment after one-pass alternate ring-groove pressing and torsion. Thus, dynamic recrystallization can proceed better and reduce the density of material defects. Proper deformation combined with proper deformation temperature can greatly improve the degree of recrystallization of the material, and increase the proportion of recrystallized structure to

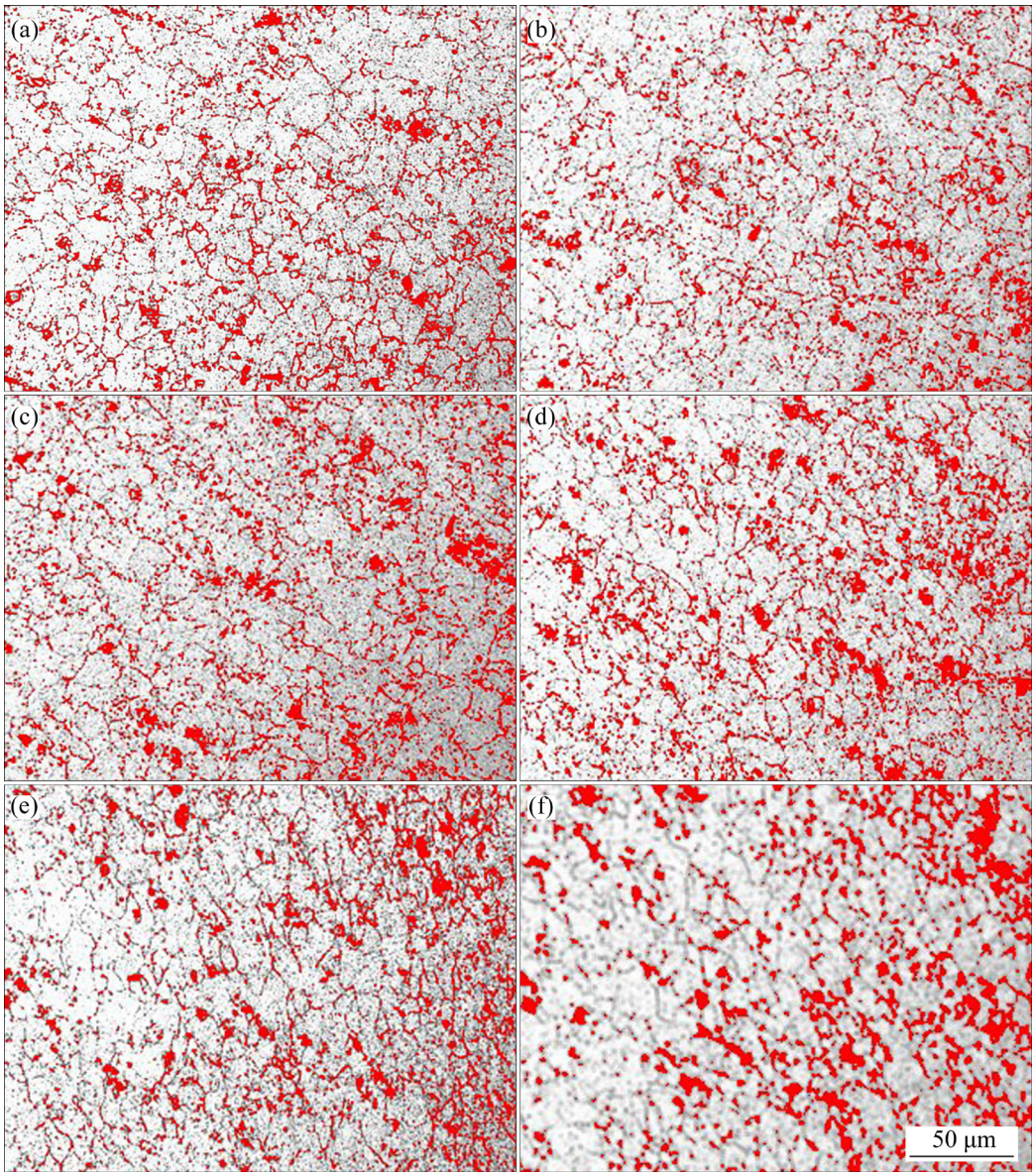

Fig. 7 Metallographic structure of sheet processed by Process 3-1: (a) Position 1; (b) Position 2; (c) Position 3; (d) Position 4; (e) Position 5; (f) Position 6

about 80%. The average grain size grows. The β phase further precipitates at the intersection point of the sub-grain boundary and grain boundary. Precipitation is also found inside the crystal grains. The location of β phase precipitation gradually expands from the grain boundary to the inside of α phase matrix as the heating temperature increases.

The metallographic structure of the sheet processed by Process 1-2 is shown in Fig. 8. Compared with one-pass deformation, the crystal grains become more equiaxed after two-pass heating and flattening at 200 °C. At this time, the main softening mechanism of the material is dynamic recovery, and a large number of sub-crystalline structures are still present. However, a small number of dynamic recrystallization structures have appeared in the material, and the overall average grain size is 12.5 μm. This finding shows that when the warm flattening temperature is low, increasing the amount of strain through strong deformation can also promote the occurrence of local dynamic recrystallization.

The metallographic structure of the sheet processed by Process 2-2 is shown in Fig. 9. Compared with the one-pass process, the number of recrystallized grains has increased, but a large number of sub-crystals are still present at the grain

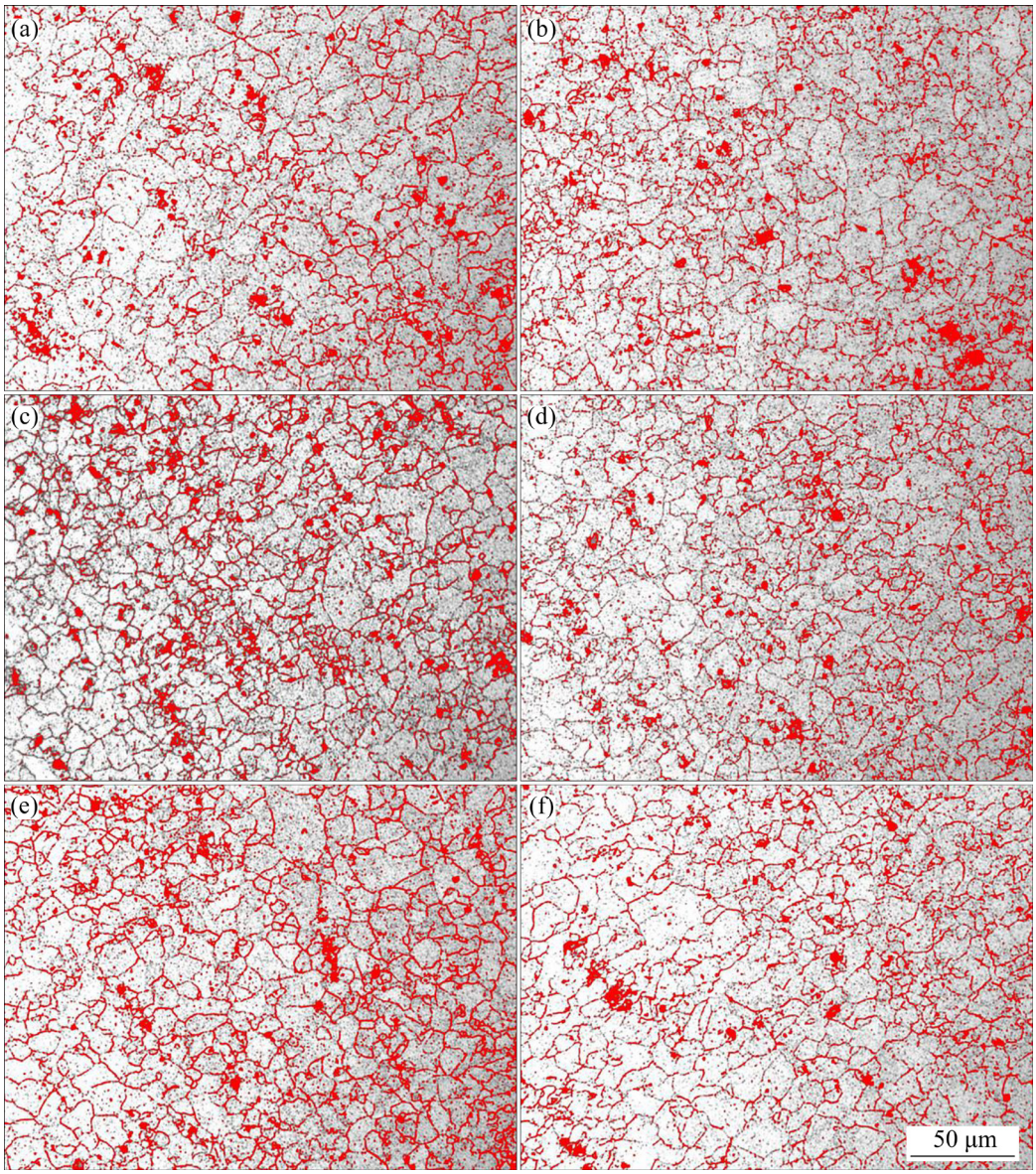

Fig. 8 Metallographic structure of sheet processed by Process 1-2: (a) Position 1; (b) Position 2; (c) Position 3; (d) Position 4; (e) Position 5; (f) Position 6

boundaries of the recrystallized grains. The size difference between the two kinds of crystal grains is relatively large; thus, a bimodal grain structure is formed. The recrystallized grain size reaches 22.8 μm.

The metallographic structure of the sheet processed by Process 3-2 is shown in Fig. 10. The precipitate amount of the second phase is obviously increased, and the recrystallization effect is obviously enhanced. This outcome is due to the large amount of torsional deformation and heating, which promotes the precipitation of the second phase and the occurrence of dynamic recrystallization. The size of the recrystallization nucleus is about 1 μm (dislocation cells, spores). Process 3-2 is a two-pass alternate ring-groove pressing and torsion and strong deformation at 300 °C. The grain refinement is more obvious and the average grain size reaches 13.5 μm because the temperature and the number of passes have increased. Grain size is remarkably refined compared with the morphology of the two-pass flattening treatment at 250 °C.

3.2 Mechanical properties

The true stress–strain curves of the sheets subjected to alternate ring-groove pressing and torsion are shown in Figs. 11 and 12. Compared

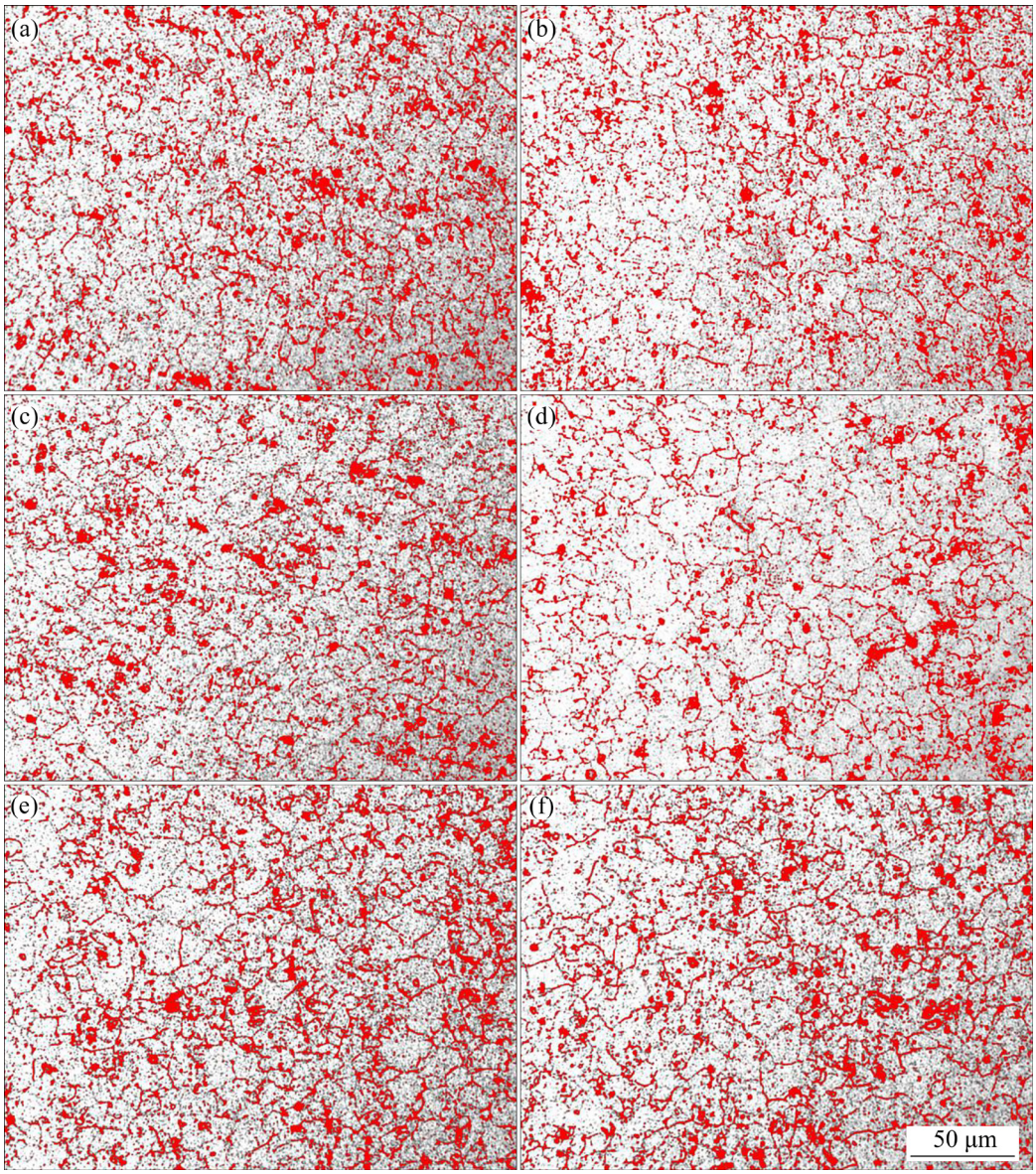

Fig. 9 Metallographic structure of sheet processed by Process 2-2: (a) Position 1; (b) Position 2; (c) Position 3; (d) Position 4; (e) Position 5; (f) Position 6

with the original sheet, the deformed sheet processed with one-pass deformation at 200 °C has a remarkable improvement in performance. Specifically, the yield strength of the sheet increased by about 110% to 233 MPa, and the tensile strength increased by about 20% to 376 MPa, but the elongation at break was unchanged. Compared with one-pass deformation, the yield strength of the deformed material after two-pass deformation reached 230 MPa, and the tensile strength decreased to 355 MPa, but the fracture elongation increased to 20.5% by a large margin. Compared with torsion at room temperature, the deformation strength after one-pass processing was greatly improved, but the elongation was the same. The deformation strength and elongation after two-pass processing were greatly improved. The result shows that the softening effect of dynamic recovery leads to the increase of elongation. Moreover, the phenomenon of strong deformation hardening leads to a slight increase in strength on the basis of high elongation compared with flattening and torsion at room temperature.

The performance of the deformed sheet processed by one-pass processing at 250 °C was markedly improved compared with the original sheet. After one-pass deformation, yield strength increased to 205 MPa, tensile strength increased by

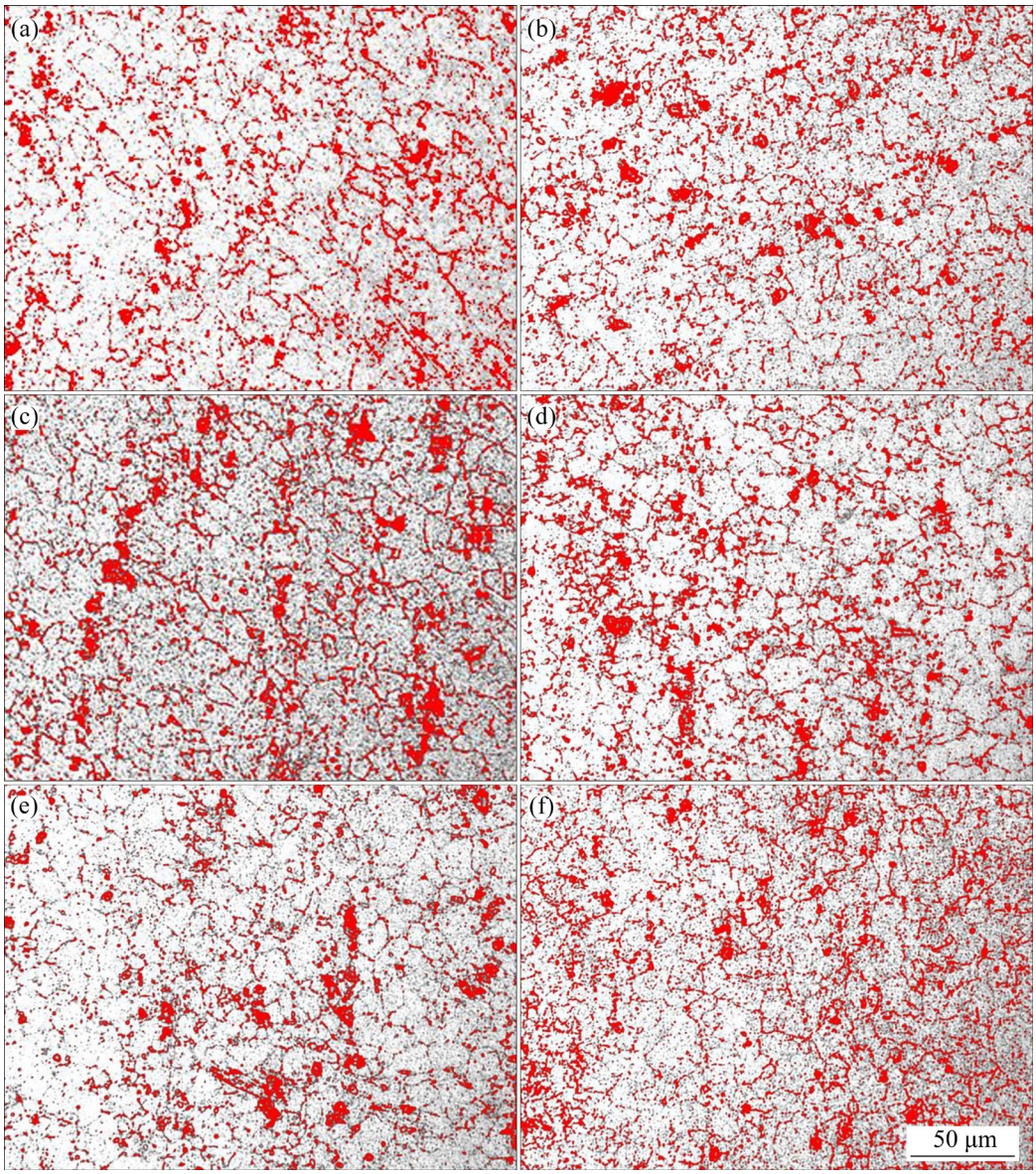

Fig. 10 Metallographic structure of sheet processed by Process 3-2: (a) Position 1; (b) Position 2; (c) Position 3; (d) Position 4; (e) Position 5; (f) Position 6

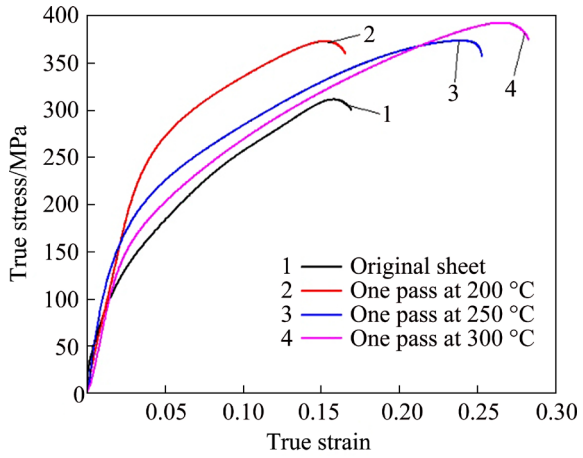

Fig. 11 True stress−strain tensile curves of one-pass alternate ring-groove pressing and torsion

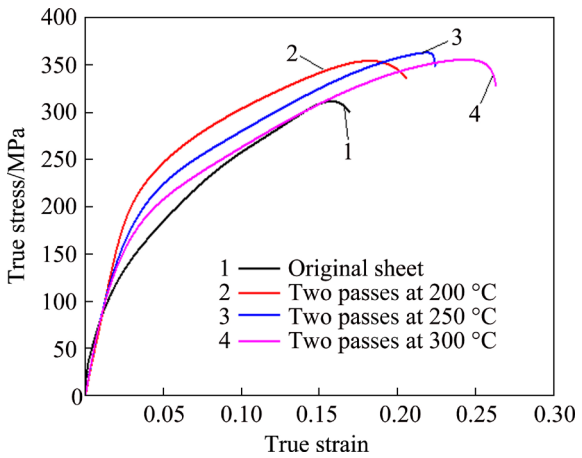

Fig. 12 True stress−strain tensile curves of two-pass alternate ring-groove pressing and torsion

about 20% to 374 MPa, and the elongation at break increased remarkably by about 45% to a value of 25.2%. Compared with one-pass deformation, two-pass deformation did not remarkably change the yield strength of the deformed sheet. The yield strength did not change much and reached 193 MPa, and the tensile strength was slightly reduced to 363 MPa. The elongation at break was reduced to 22.4%, which was still about 30% higher than that of the original material. Compared with flattening and torsion at 200 °C, the strength of the material under this process was basically unchanged and the elongation was further improved.

The performance of the deformed sheet processed by one-pass processing at 300 °C was greatly improved compared with that of the original sheet. After one-pass deformation, the tensile strength increased by about 30% to a value of 393 MPa, and the elongation at break increased substantially by about 60% to a value of 28.3%. The synergistic effect of the grain refinement strengthening and dynamic recrystallization is remarkable. Compared with the one-pass deformation, the yield strength of the sheet after two-pass deformation does not change much, and the tensile strength and elongation at break are reduced. This is mainly due to the sufficient recrystallization of the sheet under the condition of one-pass flattening at 300 °C. However, with the number of passes increasing, the effect of recrystallization on the performance of the sheet cannot be further enhanced. The comprehensive performance of the sheet that is deformed by repeated molding and torsion at 300 °C for one pass is the best compared with that of the sheet flattened and twisted by two passes at 250 °C. This is mainly because the temperature and pass make the recrystallization and strong deformation, leading to the comprehensive effect of hardening to achieve the best effect.

When the passes are the same and the temperature increases, the elongation and strength of the mechanical properties increase. It can be seen that the performance of the board is affected by the heating temperature. Dynamic recrystallization improves the microstructure morphology, thereby improving the mechanical properties of the material. Compared with the original performance, the strength of the sheet treated in the same pass has greatly been improved. But the increase in strength is not obvious as the temperature rises. The elongation of the sheet treated in the same pass has greatly been improved, and the elongation increased significantly with the increase of temperature. It can be seen that the coupling effect of temperature is of great significance for improving the strength and plasticity of materials by alternate ring-groove pressing and torsion.

3.3 Morphology of tensile fracture at room temperature

The sheet was prepared by two-pass repeated molding, torsion and flattening with ring-groove molds at different temperatures. The high magnification SEM images of the tensile fracture of the sheet are shown in Fig. 13. The dimples of the fracture are shallow and the direction of the tearing edge tends to be the same at 25 ℃. When the flattening temperature increases to 200 ℃, the dimple depth increases, and a small number of micropores accumulate near the tearing edge. When the flattening temperature increases to 250 ℃, the dimples gradually show equiaxed shape, and the number of tearing edges increases. When the flattening temperature increases to 300 ℃, the dimple presents equiaxed shape, and there are a large number of fine and uniform equiaxed micropores near the dimple, which indicates that the plasticity and toughness of the material have been improved, and it is consistent with the test results of mechanical properties [26].

Figure 14 shows the TEM microstructure of the sheet prepared by alternate ring-groove pressing and torsion at 300 ℃. It can be seen from Figs. 14(a) and (b) that a large number of fine and uniform second phases with a size between 100 and 400 nm precipitated during the processing. Figures 14(c) and (d) show the diffraction patterns of the matrix and the second phase, respectively, indicating that the second phase is $Al_6(MnFe)$. At the same time, due to the large amount of torsional deformation and the increase of deformation temperature, the recrystallization is strengthened. A large number of particles with an average size less than 1 μm are produced on the original grain boundary, but the recrystallization is still insufficient. Figure 14(e) shows the initial state of recrystallized grain formation. A large number of dislocations are generated at the grain boundary and a large number of fine subcrystals are formed. Figure 14(f) shows

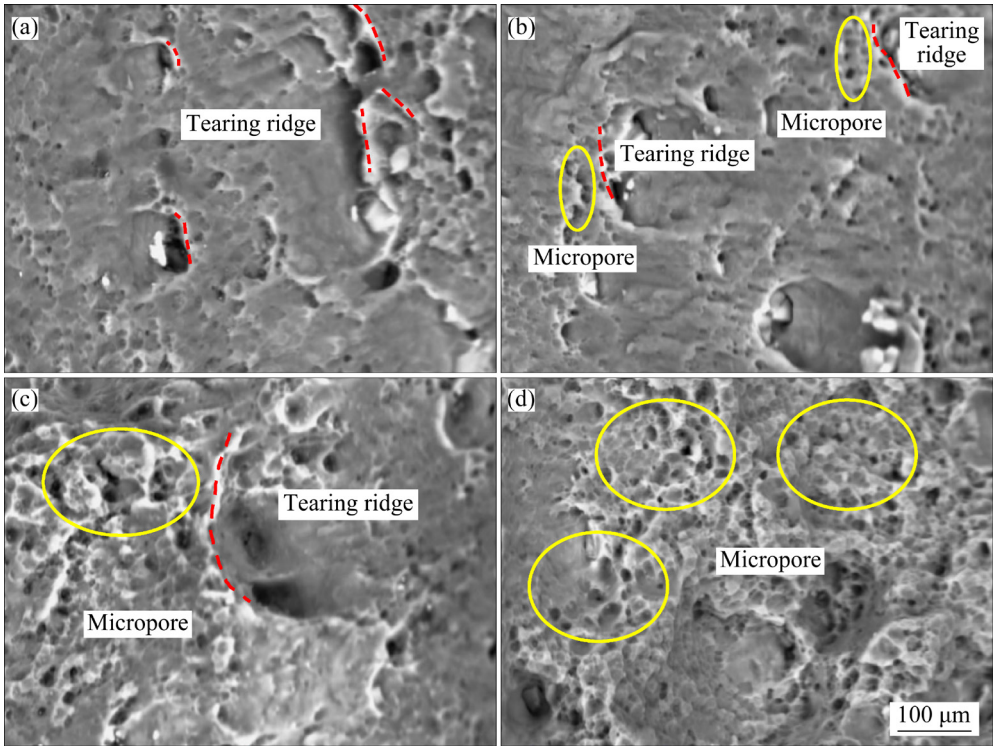

Fig. 13 High magnification SEM images of tensile fracture of sheet prepared by two-pass torsion and flattening at different temperatures: (a) 25 ℃; (b) 200 ℃; (c) 250 ℃; (d) 300 ℃

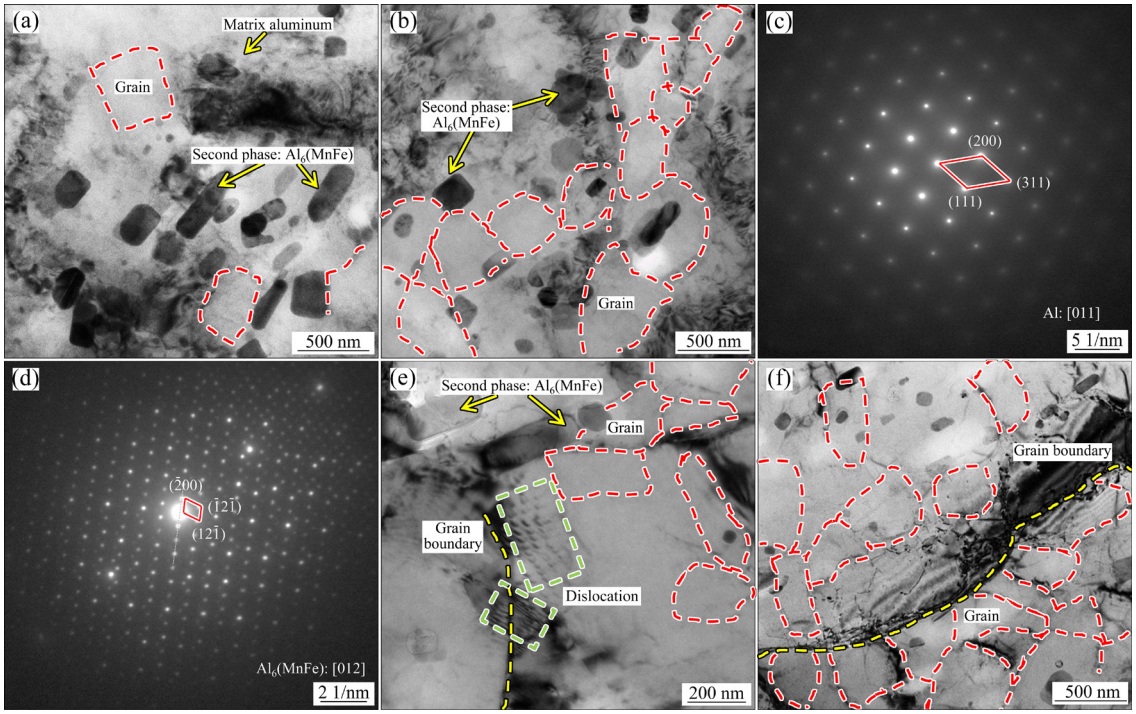

Fig. 14 Microstructure of sheet prepared by alternate ring-groove pressing and torsion at 300 ℃: (a) TEM image in initial state of processing; (b) TEM image in later period of processing; (c) Matrix diffraction pattern; (d) Second phase diffraction pattern; (e) Initial state of recrystallized grain formation; (f) Metallography of fully recrystallized sheet

that a large number of equiaxed recrystallized grains have been formed at the grain boundary. The formation of fine and uniform second phase particles and a large number of recrystallized grains can improve the strength of the material through the two effects of second phase strengthening and

fine grain strengthening [27]. At the same time, the large amount of torsional deformation and high deformation temperature promote the occurrence of recrystallization. The phase difference between the subcrystals increases and disappears, and some of them are gradually transformed into high angle grain boundaries. The migration of high angle grain boundaries removes some dislocations and promotes the occurrence of recrystallization, which improves the plasticity and toughness of the material.

4 Conclusions

(1) After plastic deformation by alternate ring-groove pressing and torsion method, the grain of 5083 aluminum alloy sheet was refined, for instance, the average grain size of the aluminum alloy was reduced from 24 to 12.5 μm before and after plastic deformation at 200 °C.

(2) The tensile strength and elongation of 5083 aluminum alloy sheet were increased for about 30% and 60%, respectively, after plastic deformation under 300 °C condition by utilizing alternate ring-groove pressing and torsion method.

(3) The formation of fine and uniform second phase particles and a large number of recrystallized grains can improve the strength of the material through the two effects of second phase strengthening and fine grain strengthening. At the same time, the large amount of torsional deformation and high deformation temperature promote the occurrence of recrystallization, which improves the plasticity and toughness of the material.

Acknowledgments

This project is financially supported by the Natural Science Foundation of Hebei Province, China (No. E2019203005).

References

[1] YOON E Y, LEE D J, PARK B, AKBARPOUR M R, FARVIZI M, KIM H S. Grain refinement and tensile strength of carbon nanotube-reinforced Cu matrix nanocomposites processed by high-pressure torsion [J]. Metals and Materials International, 2013, 19: 927−932.

[2] AAL M I A E, YOON E Y, KIM H S. Microstructure evolution and mechanical properties of Al-1080 processed by a combination of equal channel angular pressing and high pressure torsion [J]. Metallurgical and Materials Transactions A, 2013, 44: 2581−2590.

[3] ZHANG Z W, WANG J L, ZHANG Q L, SHI Q N. Producing ultrafine-grained materials by equal channel angular pressing: A review [J]. Materials Review, 2017, 31: 116−125. (in Chinese)

[4] WONGSA-NGAM J, WEN H M, LANGDON T G. Microstructural evolution in a Cu−Zr alloy processed by a combination of ECAP and HPT [J]. Materials Science and Engineering A, 2013, 579: 126−135.

[5] WANG W K, SONG Y P, GAO D S, YOON E Y, LEE D J, LEE C S, KIM H S. Analysis of stress states in compression stage of high pressure torsion using slab analysis method and finite element method [J]. Metals and Materials International, 2013, 19: 1021−1027.

[6] CHOI I C, KIM Y J, AHN B, KAWASAKI M, LANGDON T G, JANG J I. Evolution of plasticity, strain-rate sensitivity and the underlying deformation mechanism in Zn−22%Al during high-pressure torsion [J]. Scripta Materialia, 2014, 75: 102−105.

[7] HOU J, WANG J L, ZHANG Q L, SHI Q N. Status and expectation of research on accumulative roll bonding technique for producing metal matrix composite materials hybridized with reinforcing particles [J]. Materials Review, 2016, 30: 37−43. (in Chinese)

[8] SAITO Y, UTSUNOMIYA H, TSUJI N, SAKAI T. Novel ultra-high straining process for bulk materials—Development of the accumulative roll-bonding (ARB) process [J]. Acta Materialia, 1999, 47: 579−583.

[9] WANG Z S, GUAN Y J, WANG G C, ZHONG C K. Influences of die structure on constrained groove pressing of commercially pure Ni sheets [J]. Journal of Materials Processing Technology, 2015, 215: 205−218.

[10] POURALIAKBAR H, JANDAGHI M R, HEIDARZADEH A, JANDAGHI M M. Constrained groove pressing, cold-rolling, and post-deformation isothermal annealing: Consequences of their synergy on material behavior [J]. Materials Chemistry and Physics, 2018, 206: 85−93.

[11] JANDAGHI M R, POURALIAKBAR H, SHIRAN M K G, SHIRAZI, KHALAJ G, SHIRAZI M. On the effect of non-isothermal annealing and multi-directional forging on the microstructural evolutions and correlated mechanical and electrical characteristics of hot-deformed Al−Mg alloy [J]. Materials Science and Engineering A, 2016, 657: 431−440.

[12] JANDAGHI M R, POURALIAKBAR H, KHALAJ G, KHALAJ M J, HEIDARZADEH A. Study on the post-rolling direction of severely plastic deformed aluminum−manganese−silicon alloy [J]. Archives of Civil and Mechanical Engineering, 2016, 16: 876−887.

[13] POURALIAKBAR H, JANDAGHI M R, BAYGI S J M, KHALAJ G. Microanalysis of crystallographic characteristics and structural transformations in SPDed AlMnSi alloy by dual-straining [J]. Journal of Alloys and Compounds, 2017, 696: 1189−1198.

[14] KOTOBI M, HONARPISHEH M. Uncertainty analysis of residual stresses measured by slitting method in equal-channel angular rolled Al-1060 strips [J]. Journal of Strain Analysis for Engineering Design, 2017, 52: 83−92.

[15] HONARPISHEH M, HAGHIGHAT E, KOTOBI M. Investigation of residual stress and mechanical properties of equal channel angular rolled St12 strips [J]. Journal of Materials: Design and Applications, 2018, 232: 841−851.
[16] SHE X W, JIANG X Q, WANG P Q, TANG B B, CHEN K, LIU Y J, CAO W N. Relationship between microstructure and mechanical properties of 5083 aluminum alloy thick plate [J]. Transactions of Nonferrous Metals Society of China, 2020, 30: 1780−1789.
[17] DAI Q S, OU S S, DENG Y L, FU P, ZHANG J Q. Microstructure evolution and grain size model of 5083 aluminum alloy during hot deformation [J]. Materials Reports, 2017, 31: 143−146. (in Chinese)
[18] RASOULI S, BEHNAGH R A, DADVAND A, SALEKI-HASELGHOUBI N. Improvement in corrosion resistance of 5083 aluminum alloy via friction stir processing [J]. Journal of Materials: Design and Applications, 2016, 230: 142−150.
[19] SHAN Y M, LUO B H, BAI Z H. Flow stress of 5083 aluminum alloy during hot compression deformation [J]. Aluminum Processing, 2006, 172: 1−6. (in Chinese)
[20] ZHONG W M, GOIFFON E, L'ESPÉRANCE G, SUÉRY M, BLANDIN J J. Effect of thermomechanical processing on the microstructure and mechanical properties of Al−Mg (5083)/SiC_p and AlMg (5083)/Al_2O_{3p} composites. Part 1: Dynamic recrystallization of the composites [J]. Materials Science and Engineering A, 1996, 214: 84−92.
[21] YANG S L, LIN Q L. Microstructures and mechanical properties of A6N01 aluminum alloy welding joint [J]. The Chinese Journal of Nonferrous Metals, 2012, 22: 2720−2725. (in Chinese)
[22] KHELFA T, MUÑOZ-BOLAÑOS J A, LI F, CABRERA-MARRERO J M, KHITOUNI M. Microstructure and mechanical properties of AA6082-T6 by ECAP under warm processing [J]. Metals and Materials International, 2020, 26: 1247−1261.
[23] XIAO Z B, SHEN Z Y, HUANG Y C, HUANG J, ZOU T. Effect of annealing process on properties and microstructure of hot-rolled 5083 aluminum alloy [J]. Transactions of Materials and Heat Treatment, 2021, 42: 37−44. (in Chinese)
[24] VLADIMIR O, MIKHAIL S, DMITRY B. Multiscale study of morphology of the fracture surface aluminum-magnesium alloy with consecutive dynamic and gigacycle loading [J]. Procedia Structural Integrity, 2016, 2: 1063−1070.
[25] JIANG W M, ZHU J W, LI G Y, GUAN F, YU Y, FAN Z I. Enhanced mechanical properties of 6082 aluminum alloy via SiC addition combined with squeeze casting [J]. Journal of Materials Science & Technology, 2021, 88: 119−131.
[26] ZHU J W, JIANG W M, LI G Y, GUAN F, YU Y, FAN Z. Microstructure and mechanical properties of SiC_{np}/Al6082 aluminum matrix composites prepared by squeeze casting combined with stir casting [J]. Journal of Materials Processing Technology, 2020, 283: 116699.
[27] JIANG W M, FAN Z, DAI Y C, LI C. Effects of rare earth elements addition on microstructures, tensile properties and fractography of A357 alloy [J]. Materials Science and Engineering A, 2014, 597: 237−244.

环波反复模压和扭转工艺制备高性能 5083 铝合金

顾勇飞[1]，刘卫鹏[1]，郭昊山[1]，张春祥[2]，骆俊廷[1,2]

1. 燕山大学 先进锻压成形技术与科学教育部重点实验室，秦皇岛 066004；
2. 燕山大学 亚稳材料制备技术与科学国家重点实验室，秦皇岛 066004

摘　要：提出一种高性能 5083 铝合金板材的制备工艺。该工艺为温热条件下基于循环应力状态进行的反复模压−扭转强变形过程。研究表明：当温度为 200 ℃时，二次变形后晶粒细化效果最好，平均晶粒尺寸从 24 μm 细化到 12.5 μm；当温度为 300 ℃时，一次变形后板材的力学性能最好。抗拉强度(397 MPa)和断裂伸长率(28.3%)分别比原板提高 30%和 60%。第二相粒子和再结晶晶粒通过第二相强化和细晶粒强化来提高材料的强度。等轴再结晶晶粒则提高了材料的塑性和韧性。

关键词：5083 铝合金；环波反复模压和扭转工艺；循环应力状态；力学性能

(Edited by Wei-ping CHEN)